Polyhedron 51 (2013) 111-116. DOI: 10.1016/j.poly.2012.12.022

An insight into coordination ability of lithium ion toward dicyanoimidazolato anions and acetonitrile. Crystal structures of salts used in new Li-ion battery electrolytes

M. Dranka*,[a] L. Niedzicki,[a] M. Kasprzyk,[a] M. Marcinek,[a] W. Wieczorek,[a] J. Zachara[a]

Faculty of Chemistry, Warsaw University of Technology, Noakowskiego 3, 00-664 Warsaw, Poland

Fax: +48 22 628 2741

* Corresponding author. E-mail: mdranka@ch.pw.edu.pl

Keywords: Lithium, N ligands, Lithium-ion batteries, Imidazoles, Crystal structures

Abstract

New generation of imidazole-derived salts was characterized by single-crystal X-ray diffraction experiments for the first time. Herein, we present crystal structures of lithium salts containing original 4,5-dicyanoimidazolato anions substituted with trifluoromethyl, pentafluoroethyl and heptafluoropropyl groups. Studied compounds crystallize as acetonitrile–solvated dimers with four-coordinate lithium cations. Structures of crystalline materials were examined with regard to the fine properties of electrolyte providing valuable information about coordination ability of substituted 4,5-dicyanoimidazolato anions. Anions act as ditopic N donor ligands containing additional weak fluorine donor-centers. Donor nitrogen atoms of imidazole and cyano groups, show slightly lower basicity than electroneutral acetonitrile solvent molecules coordinated to lithium. Presence of bulky substituents does not alter crystal structure and close-packed arrangement is observed.

1. Introduction

The development of battery materials meets an extensive market demand for an advanced generation of lithium batteries with greater power/energy densities and improved cycle/rate life properties. Lithium ion cells seem to be quite responsive to these requirements and have been in the premium scope of multiple research groups for the last decades. Conventional Li(ion) battery consists of a graphite anode, composite cathode (with an electroactive powder as a crucial component, e.g. $LiFePO_4$) and electrolyte. The latter is a solution of lithium salt in an organic solvent or mixture of solvents which commonly includes acetonitrile. Moreover, MeCN solution is frequently chosen as a model system for preliminary characterization of electrolytes. Crystal structure analysis of crystalline solvates structures has been previously used to examine solvation interactions of MeCN with Li^+ cation [1]. Interestingly, while there is a significant list of reports on new lithium cell electrode materials, there has been very little input on new salts used in lithium electrolytes themselves [2]. Some attempts based on crystallographic studies to correlate solid state structure and properties of electrolytes have been performed though [3].

In this paper, we present results of crystal structure determination and some electrochemical investigations of three lithium salts containing novel 4,5-dicyanoimidazolato anions substituted with trifluoromethyl (LiTDI), pentafluoroethyl (LiPDI) and n-heptafluoropropyl (LiHDI) groups (Scheme 1). Even though all of the three salts show superior electrochemical performance [4,5,6], the coordination ability of dicyanoimidazolato anions toward lithium cation in presence of MeCN as a solvent remains unknown. Therefore, we performed comprehensive crystal structure analysis of crystalline acetonitrile solvates of studied lithium salts to provide valuable information necessary to understand their electrochemical properties better.

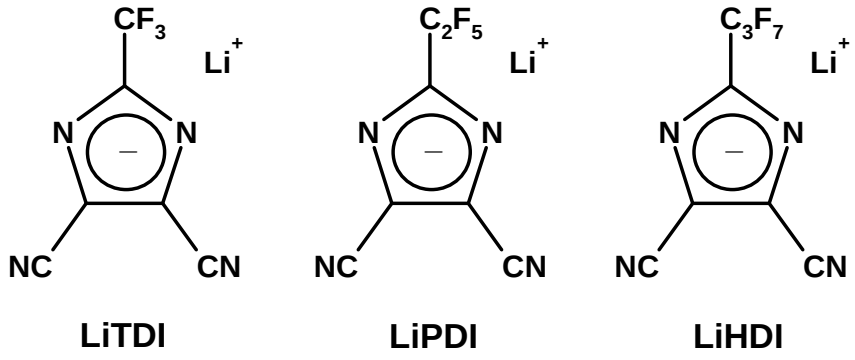

Scheme 1. Perfluorated 4,5-dicyanoimidazolato lithium salts.

2. Experimental

2.1. Preparation of salts

Series of lithium imidazole salts: LiTDI, LiPDI and LiHDI were synthesized according to the literature method [5,7]. Crystals of solvates LiTDI·2MeCN (**1**), LiPDI·2MeCN (**2**), and LiHDI·2MeCN (**3**) were obtained in drybox, under inert atmosphere of argon as follows. A 0.25 g sample of lithium salt was dissolved in 2.0 mL of anhydrous acetonitrile (Sigma-Aldrich) in a vial; then the solution was stored at room temperature for 5 days. As a result, colorless, plate-shaped, hygroscopic crystals, suitable for X-ray diffraction analysis, were grown.

2.2. Raman spectra

Raman spectra of crystalline materials were recorded with a Nicolet Almega Dispersive Raman Spectrometer in the range 100–4000 cm^{-1}. The laser source wavelength used was 532 nm.

LiTDI·2MeCN (**1**). Raman (cm^{-1}): 2994vs (CH stretching); 2278, 2256, 2241vs (CN nitrile stretching); 1498s (CC ring stretching); 1458m (CC ring stretching); 1317s (CN ring stretching); 1124w; 994w (NCN deformation); 920w (CC stretching, acetonitrile); 712w (CC ring deformation); 684w (CCN deformation); 527w (CF deformation); 492w; 380w (C1−C10 stretching + CCN bending acetonitrile).

LiPDI·2MeCN (**2**). Raman (cm^{-1}): 2995vs (CH stretching); 2278, 2256, 2238vs (CN nitrile stretching); 1489s (CC ring stretching); 1440m/w (CC ring stretching); 1309m/w (CN ring stretching); 1128w; 1043w (NCN deformation); 953m; 933w; 756w (CC ring deformation); 690w (CCN deformation); 627w; 527w (CF deformation); 389w (C1−C10 stretching + CCN bending acetonitrile).

LiHDI·2MeCN (**3**). Only a few hygroscopic crystals suitable for single crystal X-ray diffraction studies were obtained from MeCN solution, but their amount was insufficient for carrying out further analyses.

2.3. Electrochemical characterization

Conductivity measurements were performed with the Elmetron CC−401 conductometer (0.1% precision) with MI−905 Microelectrodes, Inc. microelectrode with cell constant of 1 cm^{-1} under constant stirring. The experiment was setup in a sealed 5 ml custommade bottle with the sealed ports for automatic pipette tip and thermocouple. Brand Transferpette S digital automatic pipette (10−100 μl, 0.6% precision) was used for the precise

solvent addition and heating jacket was used for thermostating. Experiment took place at low temperatures to minimize vapor pressure effect on concentration. To minimize water content influence on the conductivity, anhydrous acetonitrile was used (Sigma-Aldrich) and whole experiment was carried out in drybox (with a maximum 3 ppm water content). The experiment was arbitrarily finished at 0.26M LiTDI concentration, which is equal to 73.4:1 acetonitrile to LiTDI ratio, at which point ionic conductivity value amounts to 14.07 mS cm^{-1}.

Compound	**1**	**2**	**3**
Chemical formula	$C_{20}H_{12}F_6Li_2N_{12}$	$C_{22}H_{12}F_{10}Li_2N_{12}$	$C_{24}H_{12}F_{14}Li_2N_{12}$
M /g·mol^{-1}	548.30	648.32	748.34
crystal size /mm^3	0.45x0.4x0.3	0.3x0.3x0.1	0.3x0.2x0.05
T /K	100(2)	100(2)	100(2)
crystal system	triclinic	triclinic	Triclinic
Space group	$P\bar{1}$;	$P\bar{1}$;	$P\bar{1}$;
a /Å	8.5097 (4)	8.8408 (2)	8.9114 (4)
b /Å	8.6380 (4)	9.1778 (3)	9.2912 (6)
c /Å	10.4732 (5)	11.2039 (3)	11.7176 (8)
α/°	100.355 (4)	95.857 (3)	68.885 (6)
β /°	101.611 (4)	108.731 (3)	70.970 (5)
γ/°	113.901 (4)	117.134 (3)	61.553 (6)
V /Å^3	659.44 (5)	732.11 (4)	781.53 (8)
Z	1	1	1
D_{calc} /g·cm^{-1}	1.381	1.470	1.590
Radiation, λ/ Å	Cu K_α, 1.5418	Mo K_α, 0.7107	Mo K_α, 0.7107
μ /mm^{-1}	1.044	0.139	0.159
F(000)	276	324	372
Θ Range (°)	4.5–67.0	3.6–32.9	3.5–32.6
Reflections collected	10496	44500	21592
Independent reflections	2275	4457	4149
Obsd reflections (I>2 $\sigma(I)$)	2026	3660	3136
R_{int}	0.0357	0.0369	0.0434
Parameters/restraints	185/0	211/0	237/0
S (F^2)[a]	1.031	1.122	1.021
R1, wR2 (I>2$\sigma(I)$)[b]	0.0346, 0.0873	0.0302, 0.0847	0.0334, 0.0874
R1, wR2 (all data)	0.0403, 0.0913	0.0389, 0.0877	0.0467, 0.0905
Largest diff. peak/hole (e Å^{-3})	+0.20/−0.24	+0.45/−0.23	+0.46/−0.31

[a] Goodness-of-fit $S=\{\Sigma[w(Fo^2-Fc^2)^2]/(n-p)\}^{1/2}$ where n is the reflections number and p is the parameters number; [b] $R1=\Sigma||Fo|-|Fc||/\Sigma|Fo|$, $wR2=\{\Sigma[w(Fo^2-Fc^2)^2]/\Sigma[w(Fo^2)^2]\}^{1/2}$.

Table 1. Crystal data for the single crystal X-ray structures of 1 to 3.

2.4. Crystallographic data collection and refinement

Selected single crystals were mounted in inert oil and transferred to the cold gas stream of the diffractometer. Diffraction data were measured at 100(2) K with mirrormonochromated CuK_α (**1**) or graphite-monochromated MoK_α (**2** and **3**) radiation on the Oxford Diffraction Gemini A Ultra diffractometer. Cell refinement and data collection as well as data reduction and analysis were performed with the CrysAlis^{PRO} [8]. The structures were solved by direct methods and subsequent Fourier-difference synthesis with SHELXS−97 [9]. Full-matrix least-squares refinements against F^2 values were carried out using the SHELXL−97 [10] and OLEX2 [11] programs. All non hydrogen atoms were refined with anisotropic displacement parameters. Hydrogen atoms were added to the structure model at geometrically idealized coordinates and refined as riding atoms. The C7 methyl group in **1** and **2** exhibits orientational disorder of H atoms. An extinction correction was applied for **1** during final stages of refinement. The crystal data and experimental parameters are summarized in Table 1.

3. Results and Discussion

Crystal structure analysis of crystalline solvates provide valuable data about cation and solvent coordination that may be helpful to understand the solvation interactions present in solution. Series of lithium imidazole salts containing original 4,5-dicyanoimidazolato anions substituted with trifluoromethyl, pentafluoroethyl and heptafluoropropyl groups were crystallized as acetonitrile solvates LiTDI·2MeCN (1), LiPDI·2MeCN (2), and LiHDI·2MeCN (3). Single crystals suitable for X-ray diffraction analysis were obtained in drybox, under inert atmosphere of argon by dissolving an anhydrous lithium salt in dry acetonitrile. Colorless, hygroscopic crystals were grown in the form of plates. Attempts to crystallize lithium salts comprising a larger number of solvent molecules per Li+ cation performed at lower temperatures always result in isolation of 1–3.

3.1. Molecular structures of solvates 1−3.

Compound 1 crystallizes in the triclinic space group $P1;^{-}$. X-Ray crystal structure determination reveals a discrete dimeric species having the composition of $[Li(TDI)(MeCN)_2]_2$ shown in Figure 1. Selected bond lengths and angles are summarized in Table 2. The Li^+ cations are linked via two bridging dicyanoimidazolato ligands to give a centrosymmetric dinuclear complex in which lithium coordination environment is completed by two acetonitrile molecules.

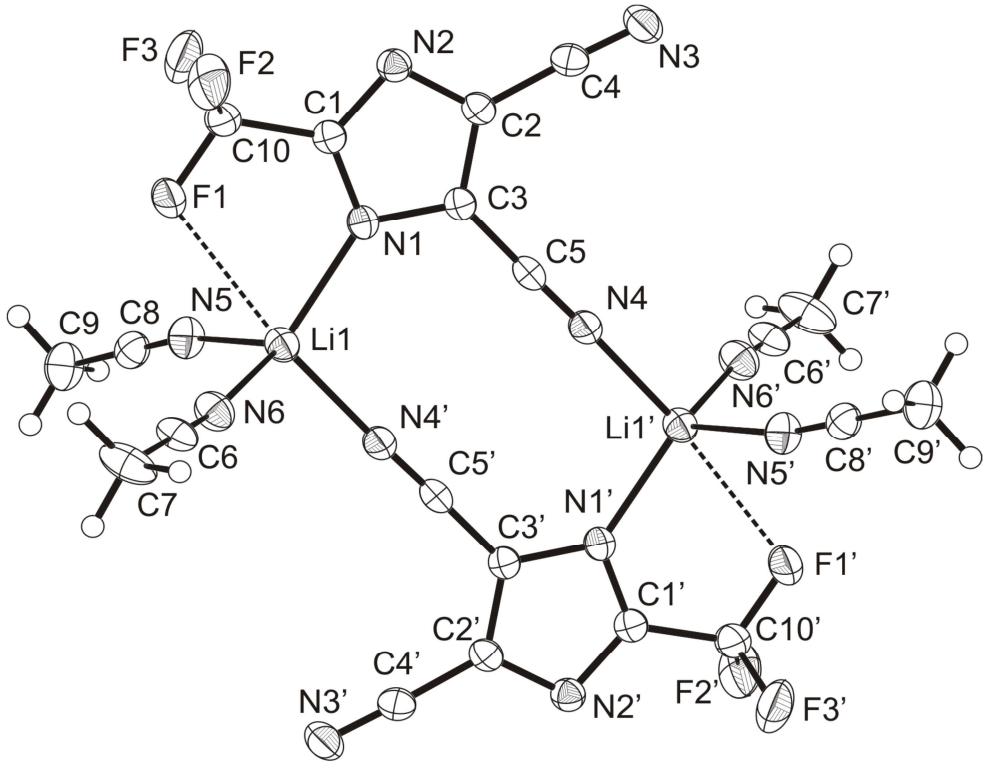

Figure 1. The molecular structure of $[Li(TDI)(MeCN)_2]_2$, compound 1, with atom numbering. Displacement ellipsoids are drawn at the 50% probability level and H atoms are shown as small spheres of arbitrary radii. Primed and unprimed atoms are related by an inversion centre.

In salt **1** TDI anion acts as a bridging ligand which is coordinated in an unsymmetrical fashion through the nitrogen atom of the imidazole ring [Li1−N1 2.071(3) Å] and one of the cyano groups [Li1'−N4 2.052(3) Å]. Consequently, two lithium atoms are doubly bridged by two NCCN sequences, forming ten-membered $Li(NCCN)_2Li$ ring around a crystallographic inversion centre. The central ring is approximately planar with r.m.s. deviations from planarity of 0.024 Å. The remaining bond lengths with acetonitrile ligands (Li1−N5 and Li1−N6) are equal to 2.043(3) and 2.011(3) Å, respectively, making average $Li-N_{(MeCN)}$ distance to be 2.027 Å). It is noteworthy that the average lithium-nitrogen(MeCN) bond length based on the data retrieved from Cambridge Structural Database for other solvates comprising two acetonitrile molecules per lithium cation is approximately 2.06 Å [12]. In comparison, $Li-N_{(MeCN)}$ bonds observed in **1** are slightly shorter and are similar to bond lengths reported for crystal structures of homoleptic lithium acetonitrile solvates (typically 1.942−2.063 Å with an average of approximately 2.02 Å) [13]. Lithium cations adopt distorted tetrahedral geometry with angles ranging from 101.68(11) to 118.19(12)°. The strongest deviation from the tetrahedral geometry is observed for acetonitrile ligands which

are bent away from the −CF3 group (N1−Li1−N6 and N1−Li1−N5 angles are equal to 118.19(12)° and 116.54(13)°, respectively). This distortion is related to an additional interaction between fluorine and lithium cation with Li1···F1 distances of 2.755(3) Å (sum of van der Waals radii for lithium and fluorine is 3.3 Å [14]). Structures containing stabilizing alkali metal···F dative bond have been reported previously [15], including complexes where Li···F interactions assist coordination of Li^+ by CF_3 group [16].

Salts **2** (LiPDI) and **3** (LiHDI), similarly as compound **1**, crystallize in the triclinic space group $P\bar{1}$. ORTEP plots of the compounds are presented in Figure 2 and selected bond lengths and angles are summarized in Table 2.

Distance/angle	**1**	**2**	**3**
Li1—N1	2.071(3)	2.0726(15)	2.095(2)
Li1'—N4	2.052(3)	2.0620(15)	2.066(2)
Li1—N5	2.044(3)	2.0278(16)	2.068(2)
Li1—N6	2.010(3)	2.0152(15)	2.0422(19)
Li1—F1	2.755(3)	2.7693(15)	2.7048(19)
N1—C1	1.3407(19)	1.3455(10)	1.3465(12)
N2—C1	1.3350(19)	1.3375(10)	1.3380(13)
N2—C2	1.3575(19)	1.3561(10)	1.3551(13)
N1—C3	1.3682(18)	1.3667(9)	1.3670(13)
C2—C3	1.389(2)	1.3911(10)	1.3934(13)
C2—C4	1.433(2)	1.4322(11)	1.4308(14)
C3—C5	1.426(2)	1.4225(10)	1.4243(14)
N3—C4	1.145(2)	1.1444(11)	1.1481(14)
N4—C5	1.1427(19)	1.1447(10)	1.1471(13)
N5—C8	1.137(2)	1.1385(11)	1.1403(14)
N6—C6	1.134(2)	1.1387(11)	1.1410(13)
C1—C10	1.494(2)	1.4938(11)	1.4953(14)
N1—Li1—N4'	106.32(12)	108.28(7)	104.54(9)
N1—Li1—N5	116.54(13)	114.41(7)	118.39(9)
N1—Li1—N6	118.22(12)	115.68(7)	114.63(9)
N5—Li1—N4'	101.66(11)	106.37(7)	110.52(9)
N6—Li1—N4'	103.65(12)	101.65(7)	100.74(8)
N6—Li1—N5	108.24(12)	109.26(7)	106.58(9)
N4'—Li1—F1	173.02(12)	173.76(7)	170.44(9)
C1—N2—C2	102.09(12)	102.32(6)	102.16(8)
C1—N1—C3	101.75(11)	101.71(6)	101.58(8)
C1—N1—Li1	127.73(12)	128.38(6)	126.36(8)
C3—N1—Li1	130.25(12)	129.53(6)	131.44(8)
C5—N4—Li1'	177.09(13)	172.48(8)	171.21(9)
C6—N6—Li1	168.02(14)	170.46(8)	173.60(10)
C8—N5—Li1	167.78(15)	167.87(8)	165.95(10)
C10—F1—Li1	109.62(10)	109.19(5)	110.21(6)
Li1—N1—C3—C5	−7.1(2)	−8.40(12)	−11.55(15)

Table 2. Selected bond lengths [Å] and angles [°] for compounds 1−3.

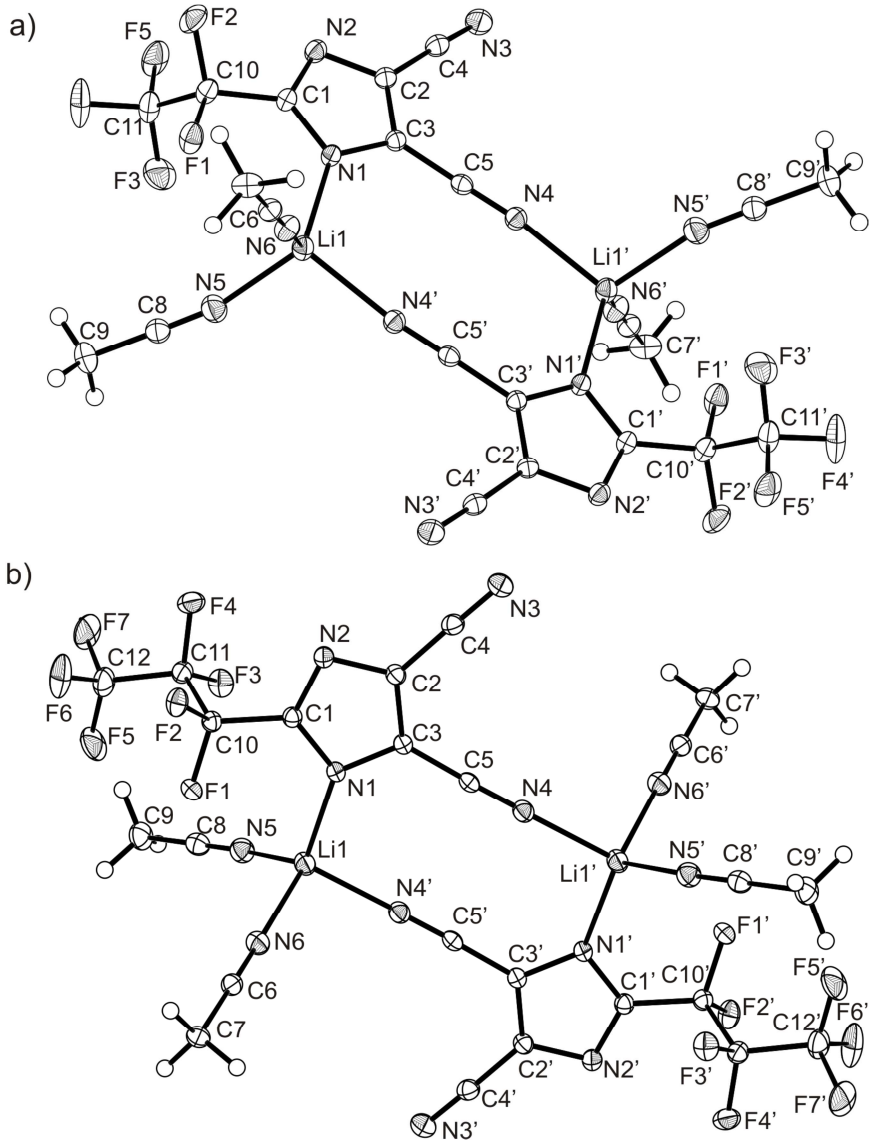

Figure 2. The molecular structure, with atom numbering, of a) [Li(PDI)(MeCN)$_2$]$_2$, compound 2; b) [Li(HDI)(MeCN)$_2$]$_2$, compound 3. Thermal ellipsoids are drawn at the 50% probability level. Symmetry code: ‘ = −*x*+1, −*y*+1, −*z*+1.

Molecular structure of salts **2** and **3** does not differ significantly from the complex **1** with regard to the coordination mode. Both compounds comprise lithium cations, dicyanoimidazolato ligands and acetonitrile solvent molecules forming together centrosymmetric dimers with ten-membered Li(NCCN)$_2$Li central rings. The r.m.s. deviations from planarity for the rings in **2** and **3** are equal to 0.051 and 0.060 Å, respectively. The bond lengths between lithium atom and acetonitrile nitrogens vary from 2.0149(16) to 2.067(2) Å and are also shorter than the bond lengths Li1–N1 with the imidazole rings (2.0726(16)–2.095(2) Å). Fluoroalkyl groups are placed out of the plane the imidazole ring. The distances

between weakly interacting lithium and fluorine atoms in **2** and **3** are equal to 2.7695(16) and 2.704(2) Å, respectively. It is worth noting that the presence of bulky perfluoroalkyl groups does not distort the dimeric molecular assembly. Steric hindrances force the central ring only slightly out of planarity, which is shown by the increase in Li1−N1−C3−C5 torsion angle (−7.1(2), −8.43(13) and −11.58(17)° for **1**, **2** and **3** respectively; see Supporting Information Figure S1). The geometry adopted by all three molecules is almost the same as pictured in Figure 3. Solely minor conformational changes can be observed for pendent acetonitrile molecules'−orientation around lithium cation.

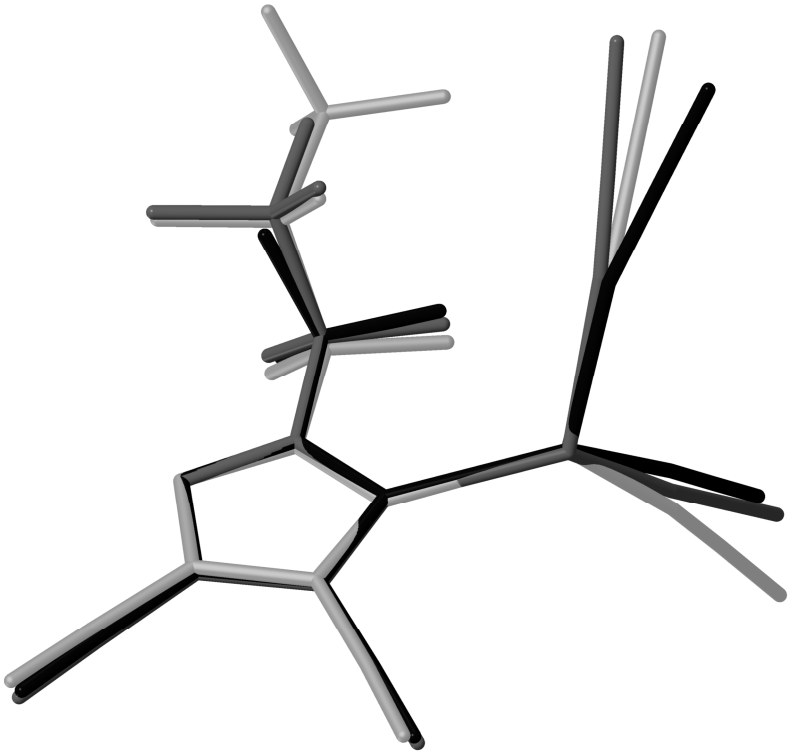

Figure 3. An overlay of the three asymmetric motifs of complexes 1 (black), 2 (dark grey) and 3 (light grey) by specifying Li1, N1, N2 atoms as geometrically equivalent.

3.2. Crystal packing of 1−3

The basic structural motif in the crystal packing of **1**−**3** is a pseudo hexagonal layer of dimeric molecules (Figure 4). There are no strong structure directing interactions present in the crystal lattices and the observed arrangement can be attributed to weak intermolecular forces.

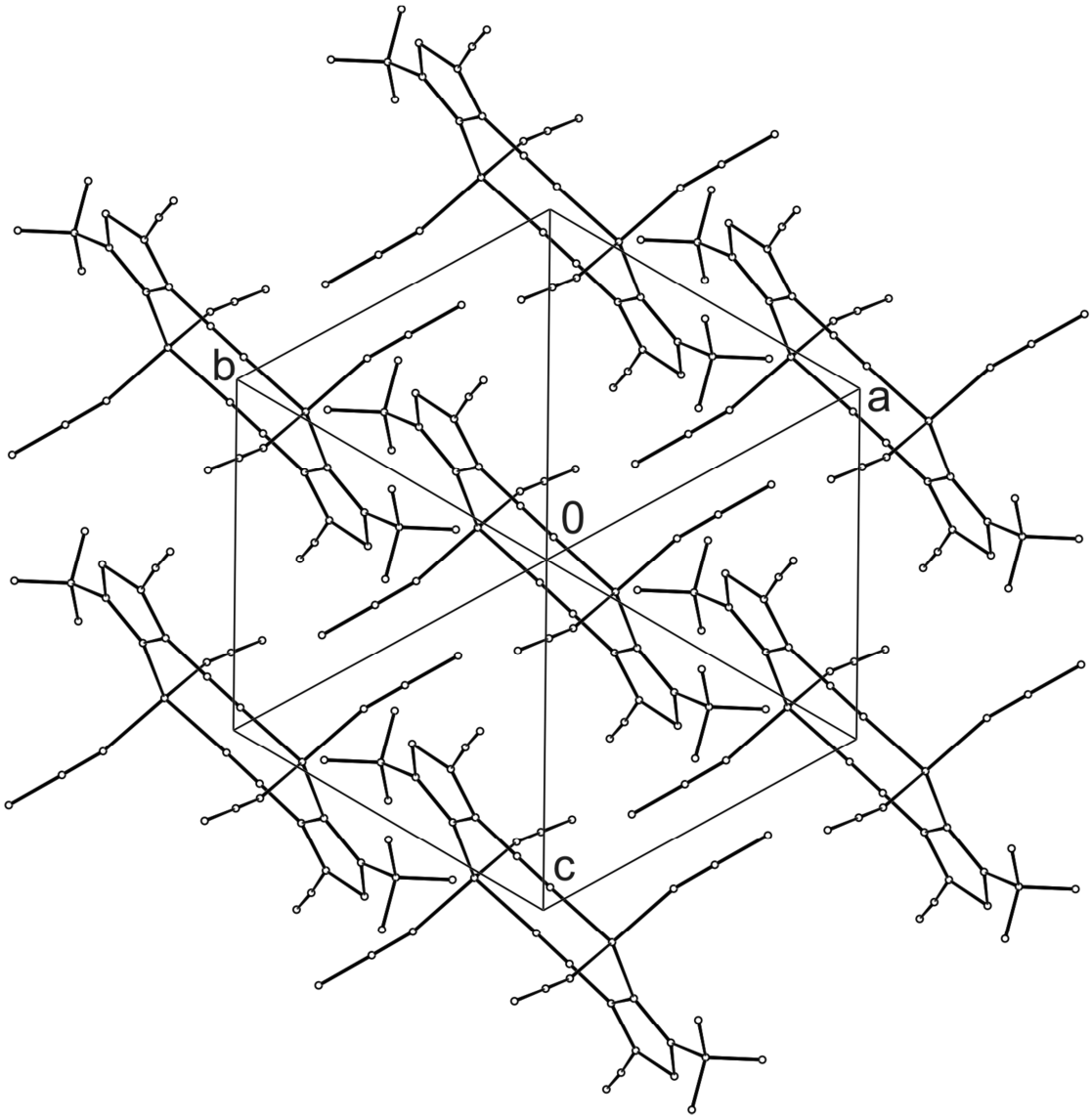

Figure 4. Projection of the crystal packing in 1 onto the (1 1 1) plane. Hydrogen atoms have been omitted for clarity.

Every dimers has six nearest neighbors in a close packed layer and three in each of the adjacent layers. Figure 5 depicts a topological illustration of this arrangement. Observed 3D layout can be described in terms of the ABC sequence of close-packed layers of spheres.

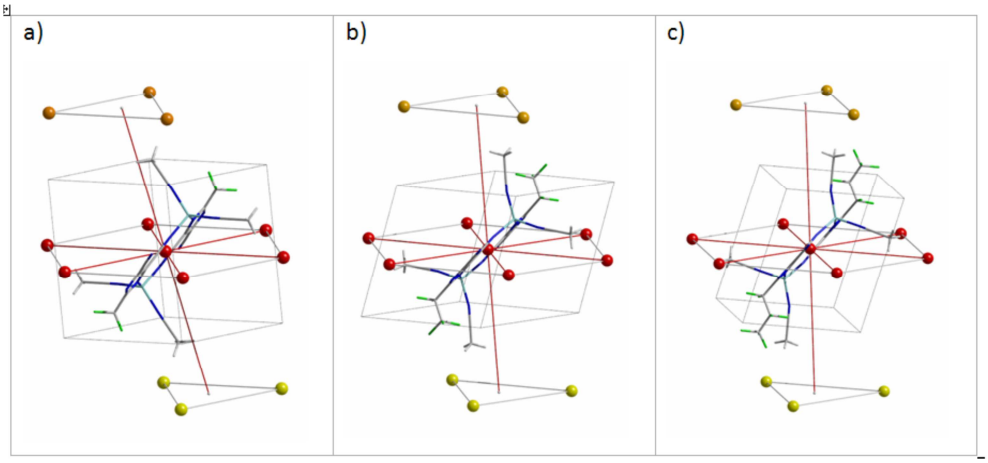

Figure 5. A topological representation of dimers arrangement in crystal lattices 1−3 resulting in pseudo-hexagonal closest packed layers. The colored balls represent centre of gravity of the dimers in a) 1, b) 2 and c) 3.

However, fluoroalkyl groups and pendent acetonitrile ligands are aligned to the gaps of the preceding layer and as a result, adjacent 2D hexagonal layers are slightly shifted with respect to one another. Slippage of the layers can be described with help of the angle between a plane parallel to the layer and the line connecting centers of stacked layers. Deviation from the ideal angle of 90° varies form 80.94(1)° for **1** through 84.93(1)° for **2** to 86.67(1)° for **3**. Increasing angle values are correlated with the elongation of structural parameters and growing cell volume: 659.44(5), 732.11(4) and 781.54 (10) Å$_3$ for **1**, **2** and **3**, respectively. Incorporating bulkier alkyl group separates sheets and almost undistorted closest packing appears. Furthermore slippage of layers is accompanied by weak intermolecular interactions. Closer inspection of packing arrangement reveals π-stacking interactions which stabilize crystal structures of **1**−**3.** Figure 6 shows chains of dimers in **1** with the imidazole rings of adjacent dimers overlapping. The chains propagate in the direction of the *Y* axis, with the Li−Li distance along the chain being equal to the *b* cell parameter, 8.6380(4) Å. Imidazole rings in the stacks are related by a centre of inversion and are parallel with a shift displacement of 1.170(3) Å. Interplanar distance of 3.530(3) Å and centroid-centroid distance 3.719(3) Å indicate medium to very weak π-stacking interactions [17].

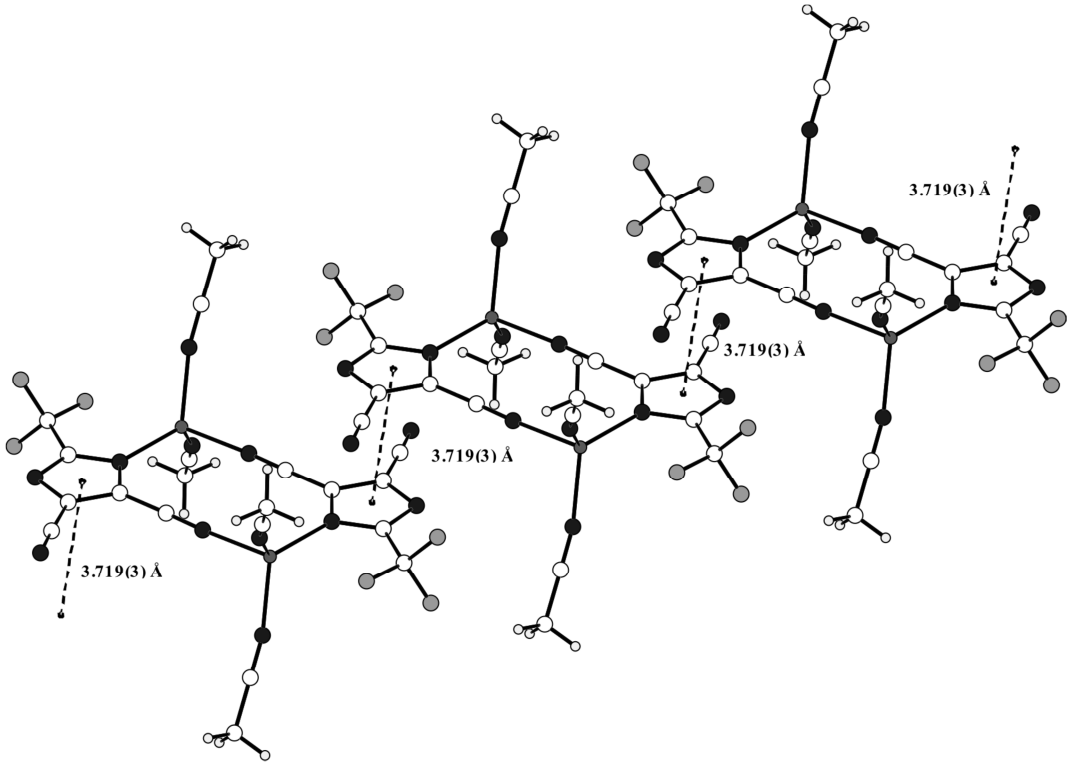

Figure 6. Depiction of centroid-centroid distance and shift displacement between two imidazole rings showing π–π interaction within the conventional π-π stabilization distance.

There is an analogous pattern of π-π contacts in crystal lattices of compounds **2** and **3**. Centroid-to-plane, centroid-to-centroid and shift displacement distances for all three compounds are summarized in Table S1 (see Supporting Information). It is noticeable that the π-π intermolecular interaction is weaker in **2** and **3** than in **1** which is probably due to the repulsion of bulkier fluoroalkyl groups. Moreover, centroid-to-plane distance of 3.697(2) Å in **3** and inter-centroid contact equals 3.845(2) Å which places this interaction close to the maximum contact distance accepted for π-π interactions.

3.3. Electrochemical properties

The results presented herein explain the superior electrochemical properties of the LiTDI type of electrolytes from the structural point of view. The fact that the coordination environment of the Li^+ cation is completed by weak intramolecular Li···Fcontacts as well as longer Li–N bonds to the imidazolato anion than electroneutral acetonitrile molecules indicates characteristic properties of trifluoromethyl dicyanoimidazolato ligand. TDI anion is a soft base with delocalized electron charge and both types of nitrogen centers in TDI act as weaker electron pair donors than acetonitrile. Furthermore, TDI can adjust its electronic properties as Lewis base and is able to fulfill the coordination sphere of lithium involving

additional fluorine-cation interactions. Smooth ligand exchange around hard lithium cation is a desirable feature for Li(ion) electrolytes to guarantee proper ion transport. Considering properties of perfluorodicyanoimidazolato anions, one can expect that dimeric ionic pairs observed in solid state dissociate in solution starting with the weakest $Li{-}N_{imidazole}$ bonds (see Scheme 2).

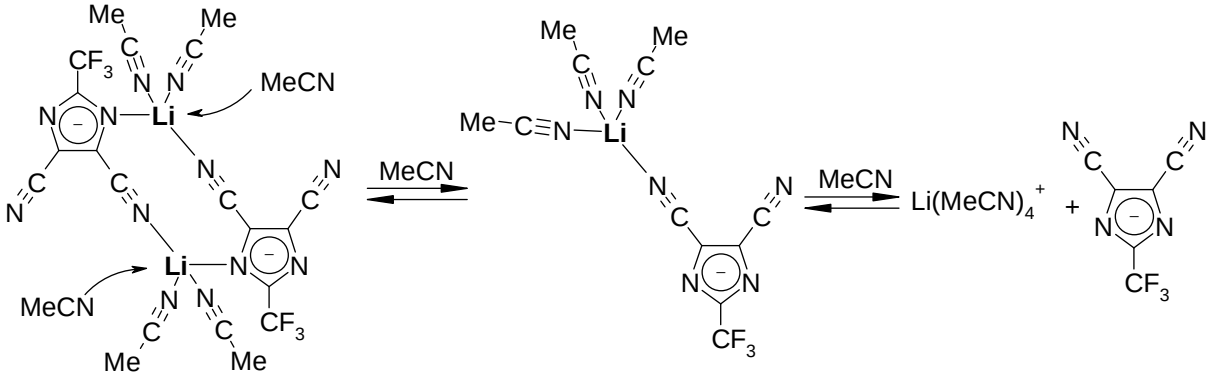

Scheme 2. Proposed solvation and dissociaton mechanism for LiTDI salt family.

This assumption agrees with conductivity measurements performed during dilution of saturated LiTDI solution in acetonitrile. Figure 7 shows concentration dependence of ionic conductivity in two temperatures. The experiments start at 19 acetonitrile moles per 1 mole of LiTDI ratio, i.e. the moment LiTDI has just been dissolved (experimenter observation). The initial increase in ionic conductivity can be explained by the dissociation of dimeric ionic pairs and formation of the solvated $Li(MeCN)_4^+$ cations (Scheme 2). Such process weakens lithium-anion ionic interactions and decreases ion agglomerates concentration which is easier to achieve in higher temperatures. Maximum of the ionic conductivity of 20.29 $mS{\cdot}cm^{-1}$ is measured at exactly 24.5 moles of acetonitrile per 1 mole of LiTDI at 25°C (22.3:1 at 28°C with 21.78 $mS{\cdot}cm^{-1}$ conductivity value). Further solvent addition only dilutes the solution decreasing the concentration of the electroactive moieties and decreasing steadily ionic conductivity. High lithium cation transference numbers and high ionic conductivity of electrolytes mostly depend on the low ionic association of the salt, which results from weak lithium-anion interactions.

Dicyanoimidazolato anions have a great potential because they can act as tetratopic soft bases with two pendent cyano groups and two imidazole nitrogens as potential donor atoms. In absence of additional donors like MeCN, for example crude solventless LiTDI,

several bonding motifs can be expected to employ all four coordinate sites around lithium cations.

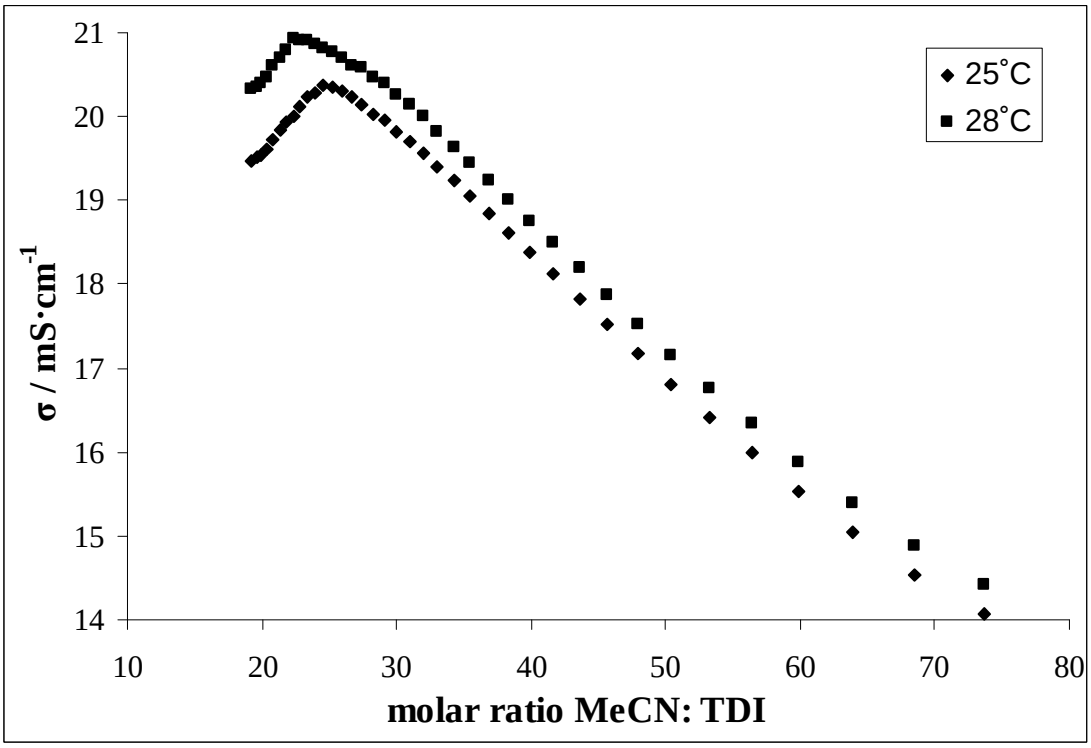

Figure 7. Concentration dependence of ionic conductivity for LiTDI solution in acetonitrile.

4. Conclusions

In summary, the formation of dimeric species in solid state is characteristic of the lithium salt incorporating 4,5-dicyanoimidazolato anions. Described anions are soft bases with highly delocalized charge and can act as potentially tetratopic N donor ligands with additional weak fluorine donor centers. Both types of nitrogen atoms, from imidazole and cyano groups, show basicity which is smaller than that of electroneutral acetonitrile solvent molecules. Structural data indicate the following series of donor centers in terms of their basicity: $N_{MeCN} > N_{cyano} > N_{imidazole}$. Introduction of bulky substituents, i.e. pentafluoroethyl and heptafluoropropyl groups, does not distort the whole crystal structure but causes only small slippage making hexagonal layers more regular and retaining close-packed arrangement in the structure. The π-π stacking interactions between imidazole rings subtly assist in establishing the molecular packing in crystal. Moreover, perfluoroalkyl substituents do not alter the electronic structure of imidazole ring and coordination ability of the entire ligand. Analysis of crystal structures suggests that dimers observed in the solid state are prevailing

species in concentrated solutions. Formation of these electroneutral dimeric adducts causes a decrease in the ionic conductivity.

Acknowledgments

This work has been supported by the Warsaw University of Technology and the Polish National Center for Research and Development Grant no. N R05 0013 06/2009.

Appendix A. Supplementary data

CCDC-879748, CCDC-879749 and CCDC-879750 contain the supplementary crystallographic data for **1**, **2** and **3**, respectively. These data can be obtained free of charge via http://www.ccdc.cam.ac.uk/conts/retrieving.html, or from the Cambridge Crystallographic Data Centre, 12 Union Road, Cambridge CB2 1EZ, UK; fax: (+44) 1223-336-033; or e-mail: deposit@ccdc.cam.ac.uk.

References:

[1] D. M. Seo, P. D. Boyle, O. Borodinc W. A. Henderson, RSC Advances, 2 (2012) 8014-8019.

[2] M. Winter, R. Brodd, Chem. Rev. 104 (2004) 4245–4269.

[3] for examples see: a) M. G. Davidson, P. R. Raithby, A. L. Johnson, P. D. Bolton, Eur. J. Inorg. Chem. (2003) 3445–3452; b) W. A. Henderson, F. McKenna, M. A. Khan, N. R. Brooks,V. G. Young, Jr., R. Frech, Chem. Mater. 17 (2005) 2284−2289; c) K. Matsumoto, R. Hagiwara, O. Tamada, Solid State Sciences 8 (2006) 1103–1107; d) Q Zhou, K. Fitzgerald, P. D. Boyle, W. A. Henderson, Chem. Mater. 22 (2010) 1203–1208.

[4] L. Niedzicki, M. Kasprzyk, K. Kuziak, G.Z. Zukowska, M. Armand, M. Bukowska, M. Marcinek, P. Szczeciński, W. Wieczorek, J. Power Sources 192 (2009) 612–617.

[5] L. Niedzicki, G.Z. Zukowska, M. Bukowska, P. Szczecinski, S. Grugeon, S. Laruelle, M. Armand, S. Panero, B. Scrosati, M. Marcinek, W. Wieczorek, Electrochimica Acta 55 (2010) 1450–1454.

[6] L. Niedzicki, S. Grugeon, S. Laruelle, P. Judeinstein, M. Bukowska, J. Prejzner, P. Szczecinski, W. Wieczorek, M. Armand, J. Power Sources 196 (2011) 8696−8700.

[7] World Patent, WO2010023413.

[8] CRYSALISPRO Software system, Agilent Technologies UK Ltd., Oxford, UK, 2012.

[9] G. M. Sheldrick, SHELXS−97, Program for solution of crystal structures, University of Göttingen, Germany, 1997.

[10] G. M. Sheldrick, Acta Crystallogr., Sect. A: Found. Crystallogr. 64 (2008) 112–122.
[11] O. V. Dolomanov, L. J. Bourhis, R. J. Gildea, J. A. K. Howard, H. Puschmann, OLEX2: A complete structure solution, refinement and analysis program. J. Appl. Cryst. 42 (2009) 339−341.
[12] F. H. Allen, Acta Crystallogr. B58 (2002) 380−388.
[13] a) D. Jacoby, C. Floriani, A. Chiesi-Villa, C. Rizzoli, J. Chem. Soc., Chem. Commun. (1991) 220-222; b) M. Hoyer, H. Hartl, Z. Anorg. Allg. Chem. 612 (1992) 45-50; c) A. Bach, M. Hoyer, H. Hartl, Z. Naturforsch., B:Chem. Sci. 52 (1997) 1497-1500; d) Y. Yokota, V. G. Young Jnr, J. G. Verkade, Acta Cryst. C55 (1999) 196-198; e) D. M. Seo, P. D. Boyle, W. A. Henderson, Acta Crystallogr. E67 (2011) m1148.
[14] A. Bondi, J. Phys. Chem. 68 (1964) 441–451.
[15] a) P. Murray-Rust, W. C. Stalling, C. T, Monti, R. K. Preston, J. P. Glusker, J. Am. Chem. Soc. 105 (1983) 3206-3214; b) J. A. Samuels, K. Folting, J. C. Huffman, K. G. Caulton, Chem. Mater. 7 (1996) 929−935.
[16] a) A. Decken, J. Passmore, X. Wang, Angew. Chem. Int. Ed. 45 (2006) 2773–2777; b) I. Krossing, H. Brands, R. Feuerhake, S. Koenig, J. Fluorine Chem. 112 (2001) 83–90; c) S. M. Ivanova, B. G. Nolan, Y. Kobayashi, S. M. Miller, O. P. Anderson, S. H. Strauss, Chem. Eur. J. 7 (2001) 503−510.
[17] C. Janiak, J. Chem. Soc. Dalton Trans. (2000) 3885−3898.